COMPUTER VISION APPLICATIONS TO THE STUDY OF SEA-ICE MOTION IN ANTARCTICA

Salvador Gutiérrez and David G. Long
Brigham Young University Microwave Earth Remote Sensing Laboratory
459 Clyde Building, Provo, UT 84602
801-378-4884, FAX: 801-378-6586, e-mail: salvador@et.byu.edu, long@ee.byu.edu

Abstract – **The motion of sea-ice in Antarctica is studied using QuikSCAT scatterometer imagery using methods from computer vision and image processing such as intensity edges and optical flow (OF). Features are computed as differential invariants based on spatial and temporal derivatives various scales. The first estimates of the motion vector field obtained through optical flow are used as the starting point for a regularization scheme that imposes constraints that bring the estimate closer to feature tracking results and observed motion. Constraints from fluid dynamics are brought in by separating the motion field into its divergence free and rotational free components with another field obtained through a convex combination of these components. The advantages of this approach are that it produces a dense motion field that can be globally processed and locally adjusted to fit data and a model. This study complements the analysis of sea ice motion by application of wavelet theory.**

I. Introduction

Sea ice has physical characteristics that make it suitable for study with microwave scatterometer and radiometer instrumentation even though these instruments were originally designed for a very different purpose [1]. Availability of large amounts of high resolution data obtained from satellite born scatterometers such as SeaWinds on QuikSCAT, has made it possible to study motion patterns of large areas of sea ice in parts of the world that are usually cloud covered or in the dark side of the earth, such as Antarctica. Among available data it is worthy to note the importance of QuikSCAT data not only for the breadth of its coverage, but for its high resolution in space and time. For these reasons QuikSCAT data are exclusively used in this study. Sea ice motion has been studied by application of a wavelet implementation of a laplacian filter ("Mexican Hat") at different scales followed by template matching [2], [3]. The proposed approach is independent of and complements wavelet approaches. As a first step, high order regularized spatial derivatives of images and time derivatives of sequences are used to compute differential invariants that define image features that follow geophysical characteristics of interest, such as coastlines, melting ice fronts and other phenomena causing intensity changes in the reconstructed radar images. These features are tracked from frame to frame with a very simple method and a sparse approximation to the motion vector field is obtained. Later, optical flow (OF) estimation methods produce an initial *dense* motion field estimate. Minimization of a regularization functional that uses the previous dense field as initial state and the sparse motion field from feature tracking as a constraint, produces a dense vector field that is closer to the observations. The additional constraints overcome the limitations of OF methods. Constraints from fluid dynamics are added at the final stage to further regularize the vector field. A convenience of this approach is that any additional information (e.g., ground truth from buoy tracking) can be easily included at any stage to constrain the regularized solution. Future research calls for a more sophisticated model based on fluid mechanics of sea ice, to be used in the last stage.

II. Scale-Space, Regularization and Features

Scale-space is a special type of multi-scale representation of a signal with a continuous scale parameter (very clear formal and informal descriptions can be found in [4]). In practice, a simple linear scale-space of an image can be generated by convolution with Gaussian kernels of increasing width. As the scale parameter grows, fine scale information is suppressed and images are smoothed until they conceivably reach a completely homogeneous intensity. In this way image information relevant to one scale is separated from unnecesary detail so the corresponding patterns can be perceived and manipulated. The amazing complexity of a huge high resolution image such as QuikSCAT imagery from Antarctica and its surrounding sea ice mantle can be conveniently broken down to discern processes that take place at different scales. Symbolically, an image represented by its intensity function $I : \mathbf{R}^2 \to \mathbf{R}$ has a scale-space generated by

$$I(x, y; s) = g(x, y; s) \star I(x, y; 0)$$

where s is the scale parameter and $g(x, y; s)$ is a Gaussian kernel with $\mu = 0$ and $\sigma = \sqrt{2s}$. Since differentiation commutes with convolution a scale-space of regularized derivatives can be generated by convolution with Gaussian derivatives

$$\partial_{x^n} I(x, y; s) = \partial_{x^n}(g(x, y; s) \star I) = g(x, y; s) \star \partial_{x^n} I(x, y; s).$$

Gaussian derivatives are regular because the Gaussian kernel is the solution to a standard regularization problem defined by Tikhonov [5]. The idea of regularization

0-7803-7536-X/$17.00 (C) 2002 IEEE

can be described using the example of the reconstruction of a signal corrupted by noise. This is an ill-posed problem with no unique solution unless a sufficient constraint can be imposed to produce a useful answer. The standard constraint is smoothness and thus we look for a signal having the desired smoothness characteristics and still fitting obervations closely enough. This compromise can be expressed as an optimization problem namely, minimizing a functional with a form

$$E[f] \equiv \frac{1}{2}\int \left((f-g)^2 + \sum_{i=1}^{\infty} \lambda_i (\frac{\partial^i}{\partial x^i} f)^2 \right) dx \qquad (1)$$

with nonnegative λ_i, where $g \in \mathcal{L}^2(\mathbf{R})$ is the signal to be regularized and f is the regularized solution. The first quadratic term of the right hand side of Eq. (1) codes for the requirement that the solution be close to the observations while the second one represents the smoothness requirement expressed as a weighted sum of squares with terms corresponding to the order of derivatives we would like the solution to have (in this case extending to infinity). It can be proved [6], that the solution to the minimization of the energy functional in Eq. (1) is a family of Gaussian kernels. Many well known differential invariants can be computed with the regularized derivatives of the images [4], for example, the Laplacian $I_{uu}+I_{vv}$ (expressed here in gauge coordinates, where v is in the gradient direction and u is orthogonal to it and $I_{uu} \equiv \frac{\partial^2}{\partial u^2}I$). Zero crossings of the Laplacian (which in terms of Gaussian derivatives is the "Mexican Hat" filter) can be used to define edges, although these lines do not always faithfully follow the contours of the true intensity borders [4]. A more faithful option is expressed by the conditions $I_{vv} = 0$ and $I_{vvv} < 0$, which may be interpreted as the maximum of the gradient in the direction of the gradient. When computed with derivatives defined at different scales this invariant results in a scale-space of edges that more faithfully follow the contours of geophysical features.

III. Estimation of sea ice motion

An initial sparse estimate of sea ice motion is derived by tracking observed ice features. This can be achieved in many ways such as template matching, but we follow a very simple method we denote as "centroid displacement vector". It consists in defining fixed sized circular neighborhoods around every pixel containing a minimum number of feature points. The centroids of feature pixels inside the neighborhood corresponding to succesive observations define a vector pointing in the general direction of the motion of pixels in the neighborhood and with a magnitude proportional to the velocity. With a proper choice of neighborhood size and minimum feature points requirement a reasonable (though sparse) motion field is obtained very rapidly. A dense first estimate of sea ice motion is derived through application of OF methods (see Fig. 1).

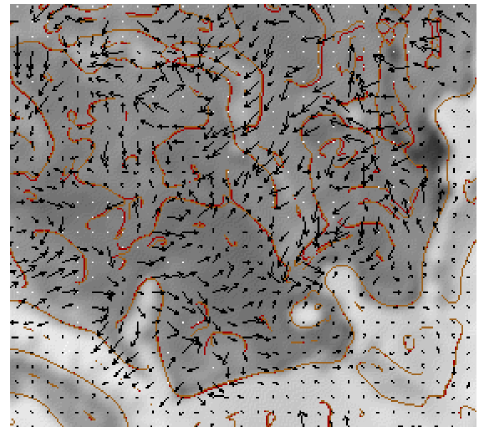

Fig. 1.
Initial OF estimation, overlaying a v-pol σ^o image of the Weddell Sea. Contour lines are feature edges.

The key relationship in these methods, usually referred to as Horn's restrictive equation [7], can be derived from the assumption that the intensity and shape of a moving neighborhood on the observed object remain invariant in a short interval.

Horn's restrictive equation can be written as a total derivative of an intensity function

$$\frac{\mathbf{D}I}{dt} = \frac{\partial I}{\partial x}\frac{dx}{dt} + \frac{\partial I}{\partial y}\frac{dy}{dt} + \frac{dI}{dt} = \nabla_s I \cdot \mathbf{u} + I_t = 0 \qquad (2)$$

where $\mathbf{u} \equiv \left(\frac{dx}{dt}, \frac{dy}{dt}\right)^T$, $I_t \equiv \frac{d}{dt}I$ and s is the scale parameter. Observe that if $\frac{\mathbf{D}}{dt}I$ vanishes, then higher order total derivatives must also vanish. In particular $\frac{d^2}{dt^2}I = 0$ which implies that $\frac{\partial}{\partial t}\nabla I \cdot \mathbf{u} + \nabla I \cdot \frac{\partial}{\partial t}\mathbf{u} + \frac{\partial^2}{\partial t^2}I = 0$.

When $\frac{\partial}{\partial t}\mathbf{u} \to 0$ and $\frac{\partial^2}{\partial t^2}I \to 0$ these relations yield a system of equations whose least squares solution yields the OF (see [8]). OF is not a very accurate estimation of the real motion field but it can be a starting point for a better estimation. Its main limitation, usually referred to as the "aperture problem" is that only the motion component in the direction of the gradient can be determined without ambiguity (see [7] and [9]). The previously computed sparse estimation from feature tracking and the dense optical flow estimation are used, respectively, to constrain and initialize an iterative procedure to minimize the following energy functional

$$\begin{aligned} E(\mathbf{u}) = \sum_{p\in L} \big[&\|\nabla I \cdot \mathbf{u}_p + I_t\|^2 \\ &+ \frac{\lambda}{|\mathcal{N}_p|}\sum_{q\in p}\|\mathbf{u}_p - \mathbf{u}_q\|^2 \\ &+ \lambda_c S(p)\|\mathbf{u}_p - c_p\|^2 \big] \end{aligned} \qquad (3)$$

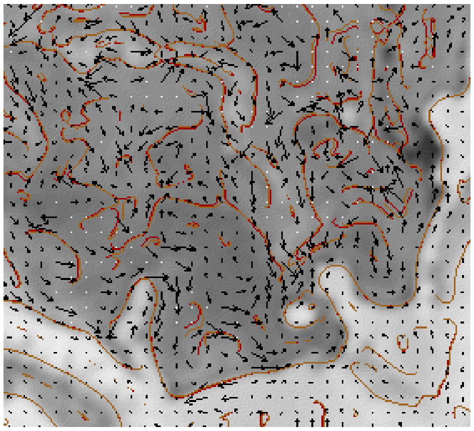

Fig. 2.
OF estimation after minimization of energy functional (3).

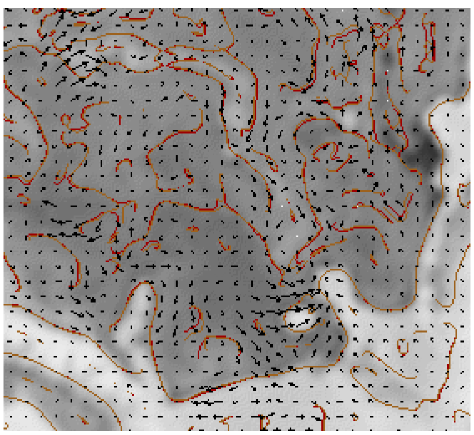

Fig. 3.
Reconstructed estimate flow.

where L is a lattice, λ and λ_c are weighting constants, $\mathcal{N}_p$ denotes the neighborhood of p and $S(p)$ is an indicator function taking the value 1 on lattice sites with a centroid displacement vector and 0 elsewhere. An example of the output of this stage is shown in Fig. 2 This functional can be minimized in a variety of ways. By setting the first variation with respect to u equal to zero, an iterative relation equivalent to Newton's method is reached. The result is a vector field that is smooth and closer to the observations. If any external information such as ground truth is available it can be included in the energy functional (3) in manner similar to data from the sparse data tracking motion field. Constraints relevant to fluid dynamics are now included via the Helmholtz decomposition

$$\mathbf{u}_p = \kappa_p + \Psi_p + \Phi_p \tag{4}$$

where p refers to a particular lattice location, Ψ_p is the divergence free component, Φ_p is the irrotational component and κ_p is a remainder harmonic component (DC). This decomposition is easily achieved in the Fourier domain, since the zero divergence flow is orthogonal to the wave number, while the irrotational flow is parallel to the wave number [10]. It is known that sea-ice motion admits a certain amount of divergent flow since ice sheets may overlap. Once the flow has been separated, a new vector field can be synthesized from a convex combination of its components, where the coefficients weigh how much of each we wish to include in the final estimation

$$\tilde{\mathbf{u}}_p = \alpha_0\kappa_p + \alpha_1\Psi_p + \alpha_2\Phi_p \tag{5}$$

where $\alpha_0 + \alpha_1 + \alpha_2 = 1$. Fig. 3 illustrates a sample result.

IV. Further research

Better ways to obtain the initial OF estimation are worth studying since they would yield a better initial estimation of the motion field. There have been some proposals that could improve on known OF limitations [9]. A sea ice flow model based on fluid dynamics can be fitted to the data using this methodology and then used for prediction and refinement of estimates.

V. Conclusion

A novel technique for sea ice motion estimation has been described. Derived from computer vision and image processing, it provides a dense estimate. It complements the study of ice motion based on wavelet analysis, allows easy inclusion of additional information as it is available, includes constraints from fluid dynamics and can lead to model based estimation, where the model would be based on fluid dynamics principles.

References

[1] D. G. Long and M. R. Drinkwater, "Cryosphere applications of NSCAT data," *IEEE Transactions on Geoscience and Remote Sensing*, vol. 37, pp. 1671–1684, May 1999.

[2] A. K. Liu, Y. Zhao, and W. T. Liu, "Sea-ice motion derived from satellite agrees with buoy observations," *Eos, Transactions, American Geophysical Union*, vol. 79, pp. 353–359, Jul 1998.

[3] A. K. Liu, S. Martin, and R. Kwok, "Tracking of ice edges and ice floes by wavelet analysis of SAR images," *J. Atmospheric and Oceanic Tech.*, 1997.

[4] B. M. ter Haar Romeny, ed., *Geometry-Driven Diffusion in Computer Vision*. P.O.Box 17, 3300 AA Dordrecht, The Netherlands: Kluwer Academic Publishers, 1994.

[5] A. Tikhonov and V. Arsenin, *Solution of Ill-Posed Problems*. Winston and Wiley, 1977.

[6] M. Nielsen, L. Florack, and R. Deriche, "Regularization and scale space," Tech. Rep. 2352, INRIA, Sep 1994.

[7] B. K. P. Horn, *Robot Vision*. The MIT Press, 1986.

[8] H. F. (Shekarforoush), "A closed-form solution for optical flow by imposing temporal constraints," in *IEEE International Conference on Image Processing*, vol. 3, pp. 656–659, 2001.

[9] M. J. Black and A. D. Jepson, "Estimating optical flow in segmented images using variable-order parametric models with local deformations," *IEEE Transactions on Pattern Analysis and Machine Intelligence*, vol. 18, pp. 972–986, Oct 1996.

[10] J. Stam, "A simple fluid solver based on the FFT," *Journal of Graphics Tools*, vol. 6, no. 2, pp. 43–52, 2001.